

## Low-spin structure of $^{96}\text{Mo}$ studied with the $(n, n'\gamma)$ reaction

S. R. Leshner,<sup>1,2</sup> C. J. McKay,<sup>1</sup> M. Mynk,<sup>3</sup> D. Bandyopadhyay,<sup>1</sup> N. Boukharouba,<sup>1</sup> C. Fransen,<sup>1,\*</sup> J. N. Orce,<sup>1</sup>  
M. T. McEllistrem,<sup>1</sup> and S. W. Yates<sup>1,2</sup>

<sup>1</sup>*Department of Physics and Astronomy, University of Kentucky, Lexington, Kentucky 40506-0055, USA*

<sup>2</sup>*Department of Physics, University of Richmond, Richmond, Virginia 23173, USA*

<sup>3</sup>*Department of Chemistry, University of Kentucky, Lexington, Kentucky 40506-0055, USA*

(Received 29 September 2006; published 27 March 2007)

Extensive studies of the low-spin excited states in  $^{96}\text{Mo}_{54}$  with the  $(n, n'\gamma)$  reaction have clarified the level scheme below 3.7 MeV excitation energy and determined detailed information about  $^{96}\text{Mo}$ , including lifetimes from the Doppler-shift attenuation method, branching ratios, and multipole mixing ratios. Also,  $B(E2)$  and  $B(M1)$  values were determined for many transitions, multiphonon states were identified, and several low-spin states were characterized in terms of collective, mixed-symmetry states.

DOI: [10.1103/PhysRevC.75.034318](https://doi.org/10.1103/PhysRevC.75.034318)

PACS number(s): 21.10.Re, 21.10.Tg, 23.20.Lv, 27.60.+j

### I. INTRODUCTION

The even- $A$  Mo isotopes show a shape change from spherical structure of the neutron closed shell nucleus  $^{92}\text{Mo}$  to the rotational, deformed structure of  $^{104}\text{Mo}$ . The nucleus studied in this work,  $^{96}\text{Mo}$ , is intermediate between these two limits. There has been considerable recent interest in this region, including the observation of shape coexistence in  $^{98}\text{Mo}$  and  $^{100}\text{Mo}$ , band crossing in  $^{100}\text{Mo}$  [1], and a transition from the  $\gamma$  soft  $^{102}\text{Mo}$  to triaxially deformed intrinsic states in  $^{104,106,108}\text{Mo}$  [2]. This shape change can be seen in the systematics of the low-lying levels presented in Fig. 1, which shows that  $^{92}\text{Mo}$  has a simple spherical structure dominated by few proton excitations, whereas  $^{104}\text{Mo}$  is clearly deformed. The  $2_1^+$  state is lowered to 192.2 keV in  $^{104}\text{Mo}$ , and  $E(4_1^+)/E(2_1^+) = 2.9$ , representing a near rotor value. Even in  $^{96}\text{Mo}$ , the transition toward deformation has begun. In this work, we investigate this structure by studying the symmetric multiphonon states as well as neutron-proton ( $np$ ) mixed-symmetry (MS) states of  $^{96}\text{Mo}$ .

An important development in this mass region was the identification of the so-called mixed-symmetry states at low energies in  $^{94}\text{Mo}$  [4–6]. This class of nuclear excitation is characterized by collective states that are not fully symmetric with respect to the  $np$  degree of freedom. Such states are predicted in the  $np$  version of the interacting boson model (IBM-2) [7–9]. A well-known example of a MS excitation is the  $1^+$  “scissors mode” excitation ( $1_{sc}^+$ ) in deformed nuclei. Since the experimental discovery of the scissors-mode excitation in  $^{156}\text{Gd}$  [10], these excitations have been identified in many nuclei, and their systematics have been well established [11,12]. The IBM-2 has attributed these states to a larger class of MS states [9]. Unlike the IBM-1, which only predicts fully symmetric states, this model allows for the exchange of distinct proton and neutron configurations in the boson wave function, giving rise to states characterized by a new quantum number,  $F$  spin, which is an approximate boson analog of

isospin [7,8]. Fully symmetric states have a maximum  $F$  spin,  $F_{\text{max}} = \frac{N_\pi + N_\nu}{2}$ , whereas MS states have  $F < F_{\text{max}}$ .  $N_\pi$  and  $N_\nu$  are the number of proton and neutron bosons, respectively, where proton and neutron pairs comprise the respective bosons.

In deformed nuclei, the  $J^\pi = 1_{sc}^+$  state, the lowest-lying MS state, is characterized by a strong  $M1$  transition to the ground state. In nearly spherical or weakly deformed nuclei, the lowest-lying MS state has  $J^\pi = 2^+$ . This state is characterized by a strong  $M1$  transition to the  $2_1^+$  state and a weak  $E2$  branch to the ground state [9].

A signature for higher lying MS states are strong  $M1$  decays to symmetric states and weakly collective  $E2$  decays to symmetric states with a strength comparable to the  $2_{ms}^+ \rightarrow 0_g^+$  transition, and stronger  $E2$  decays to the  $2_{ms}^+$  state. For two-phonon MS states resulting from the coupling of the symmetric and MS quadrupole excitations of the ground state, i.e., states with the structure  $(2_1^+ \otimes 2_{ms}^+)J^+$  for  $J = 0, 1, 2, 3, 4$ , if the boson number is large enough, collective  $E2$  decays to the  $2_{ms}^+$  one-phonon state are expected. One would expect the matrix element  $|\langle J_s | M1 | J_{ms} \rangle|$  to be  $\sim 1\mu_N$  and the  $B(E2)$  to symmetric states to be no larger than a few single-particle units.

The  $N = 52$  isotones  $^{92}\text{Zr}$ ,  $^{93}\text{Nb}$ ,  $^{94}\text{Mo}$ , and  $^{96}\text{Ru}$  have been investigated in detail and one- and two-phonon MS states were identified from  $M1$  and  $E2$  transition strengths [4–6,13–15], and recently, the study has been expanded to an odd-mass nucleus,  $^{93}\text{Nb}$  [16]. It is interesting to investigate the evolution of the characteristics of these MS states for increasing valence neutron numbers. Therefore, we have examined the  $N = 54$  nucleus  $^{96}\text{Mo}$  using the inelastic neutron scattering reaction.

The low-energy structure of  $^{96}\text{Mo}$  was studied earlier by a variety of experimental probes, which led to a fairly detailed level scheme. These methods included  $(n, \gamma)$  [17], Coulomb excitation [18], decays of  $^{96}\text{Tc}^m$ ,  $^{96}\text{Tc}$ , and  $^{96}\text{Nb}$  [19],  $(\alpha, \alpha')$  [20],  $(p, p')$  [20,21],  $(p, t)$  [22],  $(n, n')$  [23,24],  $(n, n'\gamma)$  [24], and  $(\gamma, \gamma')$  with polarized and unpolarized photons [25]. The previous  $(n, n'\gamma)$  experiment [24] concentrated on the identification of  $0^+$  states, while the present  $(n, n'\gamma)$  experiment greatly expands the level scheme, including new spin and parity assignments. The most important contributions are

\*Present address: Institut für Kernphysik, Universität zu Köln, D-50937 Köln, Germany.

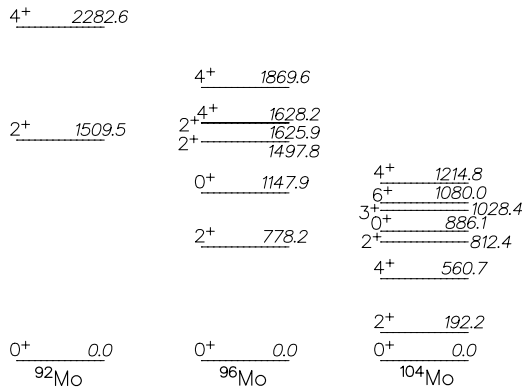


FIG. 1. Level schemes for  $^{92,96,104}\text{Mo}$  illustrating the evolution from the spherical, few-particle structure at  $^{92}\text{Mo}$  to a deformed structure at  $^{104}\text{Mo}$ . Data are from the Evaluated Nuclear Structure File of the National Nuclear Data Center [3].

the lifetime determinations. Our overall goal, then, was a more complete characterization of  $^{96}\text{Mo}$ , with special emphasis on the MS states.

A discussion of the level scheme is given in Sec. IV, multiphonon states are suggested in Sec. V, and mixed-symmetry states are discussed in Sec. VI.

## II. EXPERIMENTAL PROCEDURE

An extended set of experiments including  $\gamma$ -ray excitation functions and angular distributions were performed with the  $^{96}\text{Mo}(n, n'\gamma)$  reaction at the University of Kentucky accelerator facility, with neutron production by the  $^3\text{H}(p, n)$  reaction. The scattering sample was 40.05 g of 96.69% enriched  $^{96}\text{Mo}$  contained in a thin-walled polyethylene cylinder 5.2 cm high and 2.6 cm in diameter. The emitted  $\gamma$  rays were detected with a 50% efficient high-purity Ge (HPGe) detector, using time-of-flight gating for background suppression and a bismuth germanate (BGO) shield for active Compton suppression [26].

An excitation function measurement, providing yields as a function of neutron energy, was performed in 0.1-MeV steps from  $E_n = 2.0$  to 4.0 MeV, with the detector at an angle of  $90^\circ$  to the beam axis. Examples of the excitation functions obtained for two  $\gamma$  rays from the same level are shown in Fig. 2. Excitation function thresholds were used to place  $\gamma$  rays in the level scheme. After all  $\gamma$  rays were placed, the excitation functions were combined for each level. All normalized yields of  $\gamma$  rays cascading to a level were subtracted from the combined yields of  $\gamma$  rays from the level. These level excitation functions were then normalized to statistical model (STAT-MOD) calculations from a code modified from a published code named CINDY [27]. Cross sections for all levels were normalized with a single normalization constant. These statistical model calculations are not dependent on nuclear structure characteristics, but reflect only kinematics, spin dependencies, and neutron scattering potentials [24]. Scattering potentials were needed to properly reflect energy dependencies of scattering fields and were obtained from previous analysis in this mass region [24]. Calculated cross

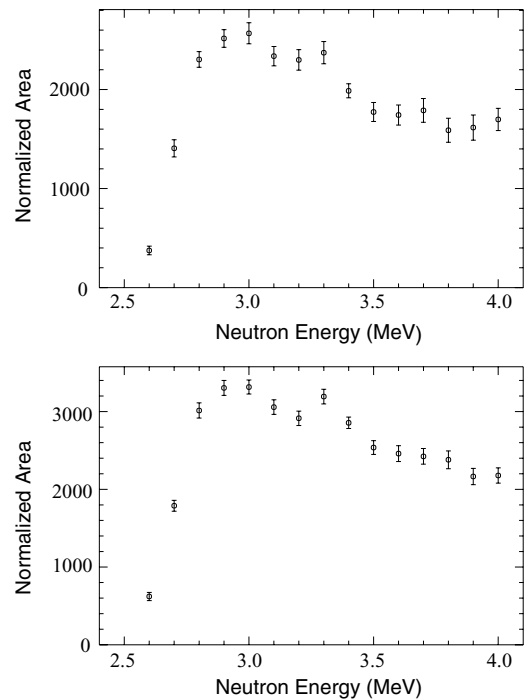


FIG. 2.  $\gamma$ -ray yields (or excitation functions) from the  $J = 1$  level at 2501.50 keV in  $^{96}\text{Mo}$ . Upper panel: yields for the 1723.29-keV transition to the  $2^+$  level. Lower panel: yields for the 1353.35-keV decay to the  $0_2^+$  level. Yields of both  $\gamma$  rays exhibit the same dependence on incident neutron energy as is necessary for transitions from the same level.

sections as a function of incident neutron energy aided in the determination of spins; an example is shown in Fig. 3.

Angular distribution measurements were also performed at incident neutron energies of 2.5, 3.0, 3.5, and 4.0 MeV over the angular range from  $40^\circ$  to  $150^\circ$ . These four neutron energies were selected to reduce feeding to the desired levels for obtaining accurate level lifetimes. A  $^{226}\text{Ra}$  source was used out of beam for energy and efficiency calibrations. In addition,  $^{60}\text{Co}$  was used during the  $E_n = 2.5$  MeV measurement as

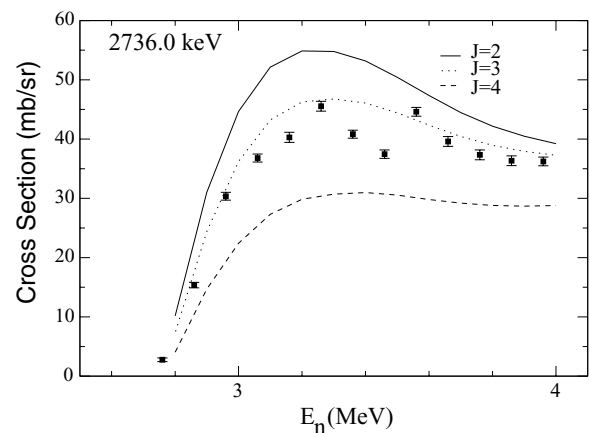


FIG. 3. Data for the level at 2735.98 keV are compared with STAT-MOD calculations for three different spin possibilities. Best fit for this level is  $J = 3$ .

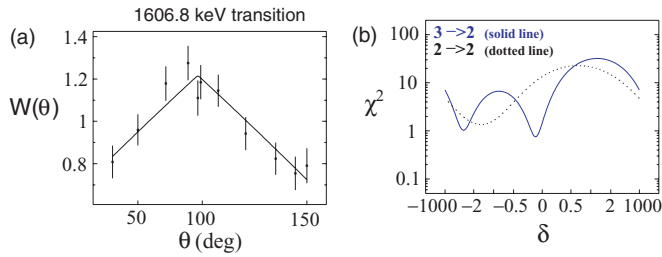


FIG. 4. (Color online) (a) Angular distribution of the 1606.8-keV  $\gamma$  ray from the 3232.45-keV level. Curve is the STAT-MOD calculation for a  $J = 3$  assignment to the level. (b) Example of the accuracy of representation of the STAT-MOD angular distribution for a transition from the 3232.45-keV,  $J = 3$  level to a  $2^+$  level as a function of the  $E2/M1$  mixing ratio (solid curve). Dotted curve represents the goodness of fit for a test of  $2^+ \rightarrow 2^+$  for the 1606.8-keV transition.

a continuous check for gain shifts. At higher neutron beam energies an additional  $\gamma$ -ray source with higher  $\gamma$ -ray energies was needed for this purpose. In this case, NaCl rings irradiated with neutrons from a  $^{252}\text{Cf}$  source were used to produce  $^{24}\text{Na}$ , which emits 1368.63- and 2754.03-keV  $\gamma$  rays after the  $\beta^-$  decay to  $^{24}\text{Mg}$ . The methods and techniques used are described in detail in other publications [26,28].

The angular distributions of the  $\gamma$  rays were fitted with even-order Legendre polynomials

$$W(\theta) = I_\gamma [1 + a_2 P_2(\cos \theta_2) + a_4 P_4(\cos \theta_\gamma)], \quad (1)$$

where the parameters  $a_2$  and  $a_4$  depend on the multipole mixing amplitudes of the transitions. These results may also be compared with STAT-MOD calculations to determine or restrict spin possibilities, as shown in Fig. 4.

These angular distribution measurements also yielded lifetimes of excited states, which were determined with the Doppler-shift attenuation method (DSAM). The  $\gamma$ -ray peaks have energies with angular dependence

$$E_\gamma(\theta_\gamma) = E_\gamma^0 [1 + \beta F(\tau) \cos \theta_\gamma], \quad (2)$$

where  $E_\gamma^0$  is the unshifted  $\gamma$ -ray energy,  $\beta$  is the initial recoil velocity in the center-of-mass frame,  $\theta_\gamma$  is the angle of observation, and  $F(\tau)$  is the Doppler-shift attenuation factor [29]. By examining the energy of a  $\gamma$  ray as a function of angle, the  $F(\tau)$  value can be determined; using the Winterbon stopping power formalism [30], the lifetime of the state,  $\tau$ , can be extracted. Examples of typical Doppler-shift curves from this work are shown in Fig. 5. Lifetimes from  $\gamma$  rays arising from the same level must match within experimental uncertainties, giving additional consistency tests of placements and aiding in the assignment of  $\gamma$  rays to specific levels.

### III. RESULTS

These experiments yielded much new information on  $^{96}\text{Mo}$ , including a wealth of  $\gamma$ -ray placements, level lifetimes, and multipole mixing ratios for decays of excited levels. New levels were found, and many were assigned spins and parities. The

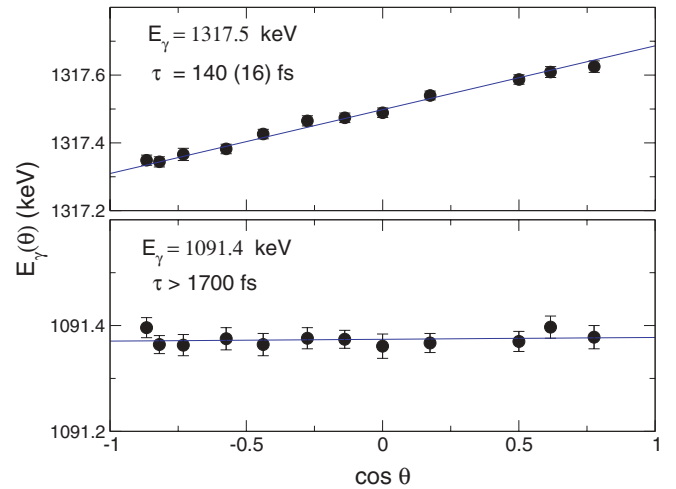


FIG. 5. (Color online) Examples of DSAM data from the  $^{96}\text{Mo}(n, n'\gamma)$  measurements. For the level emitting the 1091.4-keV  $\gamma$  ray, only a limit to the lifetime can be obtained.

comprehensive level scheme resulting from the experimental data is given in Table I. Energies listed for the  $\gamma$  rays were obtained from the angular distribution measurement at the lowest neutron bombarding energies for which the transition yields were observed to have good statistics. This procedure enabled energies to be obtained for  $\gamma$  rays which might merge into complex peak structures at higher incident neutron energies. The branching ratios and lifetimes were also obtained at the lowest feasible neutron energies. Level energies were determined by a weighted least-squares fit of all the  $\gamma$  rays from a level placed in the level scheme.

The angular distributions and level excitation functions contribute to spin assignments, but not to parity assignments directly. However, nonzero multipole mixing ratios in this work are assumed to be  $E2/M1$  ratios. If a nonzero  $\delta$  value is found, then a parity change is deemed unlikely. Magnetic quadrupole, or  $M2$ , transitions are not competitive with  $E1$  transitions nor are they common in nuclei; they are found primarily quite near closed shells. For example, the  $^{109-121}\text{Sn}$  isotopes, which have a closed proton shell, exhibit decays of this multipolarity [31]. Therefore, only  $M1$ ,  $E1$ , and  $E2$  transitions are expected in these experiments. If the multipole mixing ratio for a decay is found to be consistent with 0, within the error bars, no parity was assigned.

Transition probabilities are presented in Table II for levels whose lifetimes have been determined and are deemed to be germane to the subsequent discussion of level structure, but only have limits on their lifetimes.

### IV. DISCUSSION OF LEVEL SCHEME

Only levels for which assignments have been significantly modified from those of the Nuclear Data Sheets [32] will be discussed in this section. The  $\gamma$ -ray placements were made by considering previously placed  $\gamma$  rays and the current excitation function and lifetime measurements. Spin assignments of levels were made from angular distributions and excitation functions as described previously. In some cases, only a

TABLE I. Levels of  $^{96}\text{Mo}$  determined from the  $(n, n'\gamma)$  reaction.  $E_L$  is the level energy found in this work with uncertainties;  $I_\gamma$  is the relative  $\gamma$ -ray intensity, normalized to 1.0 for each level; from the current data, the  $\gamma$ -ray energy uncertainties are 0.05 keV unless otherwise indicated. Lifetimes  $\tau$  are mean lives. Multipole mixing ratios  $\delta$  are obtained in fits to measured angular distributions. When two values are given, they have similar  $\chi^2$  values. If one value is in brackets, the one with the smaller  $\chi^2$  is given first and is the  $\delta$  value adopted. Parentheses denote tentative assignments or placements.

$E_L$ (keV)	$J_i^\pi$	$J_f^\pi$	$E_\gamma$ (keV)	$I_\gamma$	$\tau$ (fs)	Mult	$\delta$	Notes
778.22(5)	$2_1^+$	$0_g^+$	778.28	1.00	$3670 \pm 60$	$E2$		a
1148.12(7)	$0_2^+$	$2_1^+$	369.89	1.00	$61000 \pm 8000$	$E2$		a
1497.76(5)	$2_2^+$	$2_1^+$	719.55	0.712(4)	$1070_{-360}^{+910}$	$E2/M1$	1.1(1) $0.34_{-0.7}^{+0.9}$	
1625.88(5)	$2_3^+$	$0_g^+$ $2_1^+$	1497.76 847.67	0.288(4) 0.917(2)	>1300	$E2$ $E2/M1$	$-6.9_{-2.1}^{+1.2}$ $-0.6(5)$	
1628.20(5)	$4_1^+$	$0_g^+$ $2_1^+$	1625.88 849.97	0.083(2) 1.00	$1200 \pm 200$	$E2$ $E2$		a
1869.53(5)	$4_2^+$	$4_1^+$	241.36	0.076(2)	$6100_{-1600}^{+2700}$	$E2/M1$	$-0.16(6)$ 1.5(2)	a,b
1978.42(5)	$3_1^+$	$2_1^+$ $4_1^+$	1091.38 350.05	0.924(2) 0.0852(2)	>3300	$E2$ $E2/M1$	$-0.04(3)$ $-6.1(9)$	b
		$2_3^+$	352.61	0.031(1)		$E2/M1$	0.47(6) $4.0_{-0.8}^{+1.2}$	
		$2_2^+$ $2_1^+$	480.42 1200.20	0.263(5) 0.624(6)		$E2/M1$ $E2/M1$	0.12(4) 0.89(10)	
2095.73(5)	$2_{ms}^+$	$2_1^+$	1317.50	0.985(1)	140(16)	$E2/M1$	$-0.09(2)$	
2219.35(7)	$4_3^+$	$0_g^+$ $2_2^+$	2095.59 721.77	0.015(1) 0.781(7)	>550	$E2$ $E2$		c,d
2234.63(6)	$3_1^-$	$2_1^+$ $4_2^+$	1441.05 365.13	0.219(7) 0.043(2)	>400	$E2$ $E1$		
		$2_3^+$ $2_2^+$	608.70 736.89	0.463(6) 0.449(6)		$E1$ $E1$		
2426.07(6)	$2_5^+$	$2_1^+$ $3_1^+$	1456.26 447.62	0.045(1) 0.025(1)	$270_{-40}^{+50}$	$E1$ $E2/M1$	$-2.6_{-1.6}^{+0.8}$	c
		$2_3^+$ $2_2^+$	800.22 928.24	0.358(5) 0.039(1)		$E2/M1$ $E2/M1$	$-0.18(17)$ $3.9_{-1.0}^{+1.8}$	
2438.40(12)	$5_1^+$	$2_1^+$ $0_g^+$ $3_1^+$	1647.82 2426.28 459.98	0.531(5) 0.048(2) 0.284(8)	>200	$E2/M1$ $E2$ $E2$	1.2(3)	c
		$4_2^+$ $4_1^+$	568.79 810.49	0.580(9) 0.136(6)		$E2/M1$ $E2/M1$	$-0.24(3)$ 2.4(7) 0.52(10)	
2440.39(17)	$6_1^+$	$4_1^+$	812.19	1.00	>300	$E2$		
2481.04(8)	$4_4^+$	$4_1^+$	852.86	0.750(6)	>1450	$E2/M1$	$-0.20(7)$ [1.6(4)]	e
2501.50(6)	1	$2_1^+$ $2_3^+$ $2_2^+$	1702.79 875.61 1003.69	0.250(6) 0.074(2) 0.152(3)	$140 \pm 19$	$E2$		b,e
		$0_2^+$ $2_1^+$	1353.35 1723.29	0.430(5) 0.287(4)				c
2540.34(5)	$(2^+, 3^+)$	$0_g^+$ $2_3^+$	2501.84(8) 914.52	0.057(2) 0.082(2)	$100 \pm 14$			b,d b

TABLE I. (Continued.)

$E_L$ (keV)	$J_i^\pi$	$J_f^\pi$	$E_\gamma$ (keV)	$I_\gamma$	$\tau$ (fs)	Mult	$\delta$	Notes
2594.34(6)	$3_2^+$	$2_2^+$	1042.60	0.200(4)	$1220_{-580}^{+6200}$	$E2/M1$	0.12(7)	e
		$2_1^+$	1762.09	0.718(5)				
		$3_1^+$	615.35	0.313(6)				
		$4_1^+$	966.29	0.195(6)				
		$2_3^+$	968.54	0.309(6)				
2611.53(13)	$0^+$	$2_2^+$	1096.62	–	$>280$	$E2/M1$	1.1(2)	b
		$2_1^+$	1816.14	0.183(3)				
		$4_1^+$	983.32	1.0				
		$2_1^+$	1844.25	1.0				
		$4_3^+$	405.95	0.160(7)				
2622.48(7)	$0^+$	$2_1^+$	1844.25	1.0	$840_{-300}^{+870}$	$E2$		g
2625.23(8)	$4_5^+$	$4_3^+$	405.95	0.160(7)	$690_{-270}^{+1090}$	$E2/M1$	$-0.37(16)$	
2700.08(8)	$2_6^+$	$2_1^+$	1846.98	0.840(7)	$150 \pm 20$	$E2$	$-0.11(5)$	e,h
		$2_3^+$	1074.05	–		$E2/M1$		
		$2_2^+$	1202.43	0.470(7)		$E2/M1$		
		$2_1^+$	1921.78	0.379(6)		$E2/M1$		
2734.61(12)	$4_6^+$	$0_g^+$	2700.88(16)	0.152(8)	$>360$	$E2$	$0.23(6)$	c
		$4_2^+$	865.00	0.361(14)				
		$4_1^+$	1106.47	0.639(14)				
2735.98(6)	$3_3^+$	$2_2^+$	1238.17	0.362(6)	$175_{-25}^{+26}$	$E2/M1$	$-0.34(4)$	e
2749.71(9)	$0^+$	$2_1^+$	1957.78	0.638(6)	$240_{-43}^{+54}$	$E2/M1$	$0.02(4)$	c,g,i
		$2_2^+$	(1250.78)	0.245(7)				
		$2_1^+$	1970.47	0.755(7)				
2755.12(30)	$6_2^+$	$4_1^+$	1126.91	1.00	$>280$	$E2$		
2787.07(8)	$2_7^+$	$2_3^+$	1161.29	0.045(4)	$210_{-42}^{+56}$	$E2/M1$	$-0.41_{-0.60}^{+0.30}$	c
		$2_2^+$	1289.32	0.078(4)		$E2/M1$	$1.1(10)$	c
		$2_1^+$	2008.82	0.877(6)		$E2/M1$	$-0.24(5)$	
2790.24(7)	(2,4)	$3_1^-$	555.48(7)	0.067(5)	$>980$		$5.8_{-1.3}^{+2.1}$	e
		$2_3^+$	1164.43(27)	0.349(7)				
		$2_2^+$	1292.99	–				
		$2_1^+$	2011.98	0.585(8)				
2794.34(8)	$1_1^+$	$2_2^+$	1296.63	0.192(11)	$45 \pm 5$	$E2/M1$	$-0.14(6)$	c,g,i,j
		$2_1^+$	2016.54(10)	0.114(7)		$E2/M1$		
		$0_g^+$	2794.24	0.694(16)		$M1$		
2806.23(8)	1	$2_3^+$	1180.42	0.086(3)	$165_{-26}^{+31}$			c,g,i
		$2_2^+$	1308.39	0.145(5)				
		$0_2^+$	1658.10	0.769(6)				
2818.53(10)	$4_7^+$	$4_1^+$	1190.32	1.0	$85_{-17}^{+23}$	$E2/M1$	$-0.14(6)$	
2975.41(12)	4	$3_1^-$	740.59	0.598(12)	$>500$			b,e
		$4_1^+$	1347.26	0.402(12)				
2986.79(6)	$2_8^+$	$2_{ms}^+$	891.03	0.186(7)	$150_{-20}^{+21}$	$E2/M1$	$-0.26(11)$	e
		$3_1^+$	1008.30	0.101(5)		$E2/M1$	$-0.31(16)$	c
		$2_3^+$	1360.91	0.322(8)		$E2/M1$	$3.1_{-1.2}^{+3.2}$	
		$2_3^+$	1360.91	0.322(8)		$E2/M1$	$-0.69(13)$	
		$2_1^+$	2208.55	0.268(8)			$E2/M1$	$-5_{-1}^{+2}$
		$2_1^+$	2208.55	0.268(8)		$E2/M1$	$-0.16(8)$	

TABLE I. (Continued.)

$E_L$ (keV)	$J_i^\pi$	$J_f^\pi$	$E_\gamma$ (keV)	$I_\gamma$	$\tau$ (fs)	Mult	$\delta$	Notes
							4(2)	
3006.42(9)	$0_3^+$	$0_g^+$	2986.76	0.123(15)		$E2$		c
3024.47(6)	$2_9^+$	$2_2^+$	1508.65	1.00	$130_{-22}^{+27}$	$E2$		b,k
		$3_1^+$	1045.80	0.165(7)	$120_{-17}^{+19}$	$E2/M1$	$-0.32_{-0.32}^{+0.16}$	
							-1.9(1)	
		$4_2^+$	1155.64	0.089(3)		$E2$		
		$4_1^+$	1396.26	0.428(8)		$E2$		
		$2_3^+$	1398.36	0.317(7)		$E2/M1$	-0.48(10)	
3053.20(10)	$(4^+)$	$4_1^+$	1424.99	1.00	$100_{-16}^{+20}$			
3087.70(11)	$3_4^+$	$2_{ms}^+$	992.18	0.210(10)	$480_{-200}^{+770}$	$E2/M1$	0.11(10)	e
		$4_1^+$	1459.36	0.434(10)		$E2/M1$	-1.4(2)	
							-0.52(10)	
		$2_3^+$	1461.64(6)	0.358(10)		$E2/M1$	-2.9(7)	
3089.65(9)	2,3	$2_2^+$	1591.89	0.667(11)	$95_{-12}^{+14}$			b,g
		$2_1^+$	2311.29(7)	0.333(11)				c
3134.50(7)	$2_{10}^+$	$2_3^+$	1508.65	0.499(44)	$110 \pm 14$	$E2/M1$	2.6(6)	e,i,k
		$0_g^+$	3134.50(7)	0.501(44)		$E2$		c
3154.13(46)	1	$2_1^+$	2375.88(11)	1.00	$105_{-13}^{+14}$			b,g
3178.74(7)	$3_2^-$	$3_1^-$	944.10	0.134(6)	$205_{-30}^{+35}$	$E2/M1$	-0.31(12)	b,e
		$2_{ms}^+$	1082.81(9)	0.053(5)		$E1$		c
		$2_2^+$	1680.87	0.164(6)		$E1$		c
		$2_1^+$	2400.54	0.649(10)		$E1$		
3211.35(9)	$3_5^+$	$3_1^+$	1232.94	0.314(11)	$150_{-26}^{+32}$	$E2/M1$	$2.4_{-0.6}^{+1.0}$	c,g
							-0.22(12)	
		$4_2^+$	1341.70	0.260(11)		$E2/M1$	1.8(13)	c
		$2_2^+$	1713.58	0.271(10)		$E2/M1$	$-5.2_{-2.7}^{+1.3}$	c
		$2_1^+$	2433.27(6)	0.155(8)		$E2/M1$	0.41(10)	c
							$5.4_{-2}^{+5}$	
3232.45(10)	3	$2_3^+$	1606.80	0.612(13)	$340_{-90}^{+15}$			c,g
		$2_1^+$	2454.13	0.388(13)				c
3255.60(18)		$2_3^+$	1629.66(6)	0.564(20)	$500_{-230}^{+1350}$			c,g
		$2_1^+$	2477.40(6)	0.436(20)				c
3284.89(17)	$2_{11}^+$	$2_1^+$	2506.64	1.00	$180_{-36}^{+56}$	$E2/M1$	$-1.5_{-1.6}^{+0.6}$	
3300.56(5)	$1_2^+$	$2_2^+$	1802.81	0.087(15)	$12 \pm 2$	$E2/M1$		c,g,i,j
		$0_g^+$	3300.08	0.913(15)		$M1$		c
3327.87(25)	1	$2_1^+$	2549.70(8)	0.288(36)	$70_{-14}^{+18}$			c,g,i
		$0_g^+$	3327.71(9)	0.712(36)				c
3335.24(11)	$(3^+)$	$4_1^+$	1706.54	0.190(7)	$180_{-40}^{+50}$			c,e
		$2_3^+$	1709.72	0.399(9)				
		$2_1^+$	2557.25	0.410(10)				c
3352.01(12)	$2_{12}^+$	$2_{ms}^+$	1255.75(8)	0.363(18)	$52_{-12}^{+15}$	$E2/M1$	$-0.10_{-0.28}^{+0.13}$	c,g,i
		$2_2^+$	1854.35	0.370(18)		$E2/M1$	$-1.5_{-0.8}^{+0.4}$	c
		$0_g^+$	3351.04(13)	0.268(18)		$E2$		c
3363.92(28)		$2_1^+$	2585.68(28)	1.00	$170_{-45}^{+73}$			g
3374.09(12)	$2_{13}^+$	$2_3^+$	1748.26	0.282(11)	$33 \pm 4$	$E2/M1$	$3.4_{-1.2}^{+2.9}$	c
							$-0.12_{-0.38}^{+0.14}$	
		$2_1^+$	2595.47(7)	0.718(11)		$E2/M1$	-0.51(8)	c
3416.82(13)	$4_7^+$	$2_{ms}^+$	1320.77	0.301(13)	>880	$E2$		b
		$2_2^+$	1919.36	0.386(13)		$E2$		

TABLE I. (Continued.)

$E_L$ (keV)	$J_i^\pi$	$J_f^\pi$	$E_\gamma$ (keV)	$I_\gamma$	$\tau$ (fs)	Mult	$\delta$	Notes
3421.32(12)	1	$2_1^+$	2638.55(6)	0.313(13)	$75_{-12}^{+13}$	E2		b
		$2_3^+$	1795.49	0.331(43)				c,e
		$0_g^+$	3421.00(6)	0.669(43)				c
3424.86(26)	$1_3^+$	$2_1^+$	2646.87(15)	0.071(16)	$12_{-3}^{+4}$	E2/M1		c,e,i,j
		$0_g^+$	3424.73(7)	0.929(16)		M1		c
3433.58(25)	$4_8^+$	$2_1^+$	2655.32(6)	1.00	$140_{-25}^{+30}$	E2		c,g
3441.97(17)	$4_9^+$	$2_1^+$	2663.71	1.00	$250_{-60}^{+90}$	E2		
3464.63(12)	3	$4_2^+$	1595.09	0.546(12)	$63_{-9}^{+10}$			c,g
		$2_2^+$	1966.82(6)	0.454(12)				c
3472.18(29)	$2_{-14}^+$	$2_1^+$	2693.92(7)	1.00	$95_{-20}^{+27}$	E2/M1		c
3530.67(12)	1,2,3	$2_3^+$	1904.72	0.523(11)	$62_{-8}^{+9}$			c,g
		$2_2^+$	2033.67(12)	0.477(11)				c
3540.80(14)	3	$4_2^+$	1671.48	0.366(19)	$120_{-25}^{+32}$			c,g
		$2_1^+$	2762.40	0.634(19)				b
3573.46(19)	(1)	$2_3^+$	1947.69	0.474(59)	$125_{-26}^{+34}$			c,g
		$0_g^+$	3572.88(10)	0.526(59)				c
3599.56(28)	$1^-$	$2_1^+$	2821.30(7)	0.217(59)	$15 \pm 3$	E1		c,g,i,j
		$0_g^+$	3599.45(24)	0.783(43)		E1		c
3610.46(24)	2,3	$2_2^+$	2112.94(8)	0.761(16)	$150_{-25}^{+30}$			b,g
		$2_1^+$	2831.93(8)	0.239(16)				b
3623.17(29)	$(3^+)$	$2_1^+$	2844.91(7)	1.00	$> 340$			c,g
3668.51(16)	$3_6^+$	$4_1^+$	2041.36(14)	0.478(27)	$64_{-11}^{+13}$	E2/M1	$-3.8_{-5.2}^{+1.5}$	c,g
		$2_1^+$	2890.16	0.522(22)		E2/M1	$-0.45_{-0.16}^{+0.11}$	c
							$-1.19_{-0.39}^{+0.95}$	

<sup>a</sup>Lifetime value taken from Ref. [32].

<sup>b</sup> $\gamma$ -ray placement changed from Ref. [32].

<sup>c</sup> $\gamma$  ray placed in this work.

<sup>d</sup>This peak is an unresolved doublet.

<sup>e</sup>There is a change in spin assignment from that given in the Nucl. Data Sheets [32].

<sup>f</sup>The  $\gamma$  ray is mixed with a laboratory background line and cannot be separated.

<sup>g</sup>Level unreported in Ref. [32].

<sup>h</sup>The  $\gamma$  ray is mixed with a contaminant.

<sup>i</sup>The level and/or spin identified in Ref. [37].

<sup>j</sup>Parity assignment established in Ref. [25].

<sup>k</sup> $\gamma$  ray has been multiply placed in this table.

range of spins is given as we were unable to make a unique assignment.

**1330-keV level:  $0^+$**

A level has been proposed at this energy from only a  $^{94}\text{Zr}(^3\text{He},n)$  reaction study [32]. We found no evidence of this level; a search for possible decay paths to or from this proposed level was unsuccessful. It is very unlikely that we would not observe a level at this excitation energy, therefore, we have removed the 1330-keV level from the  $^{96}\text{Mo}$  level scheme.

**1869.53-keV level:  $4^+$**

The Nuclear Data Sheets [32] assign a  $\gamma$  ray of 241.38 keV to two different levels. From the results of a  $\gamma\gamma$  coincidence measurement following the  $\beta^-$  decay from  $^{96}\text{Nb}$  to  $^{96}\text{Mo}$ ,

this level was placed at 1869.53 keV [33] and a  $(\alpha,2n)$  measurement [34] agreed with this placement. In a  $(n,\gamma)$  experiment [17], this  $\gamma$  ray was placed from levels at both 1869.53 and 2219.35 keV. The author of the compilation for  $^{96}\text{Mo}$  [32] accepted the latter multiple placement. From excitation thresholds, our data are in accord with the previous 1869.53-keV level assignment, since the  $\gamma$  ray is present at a neutron energy of 2.1 MeV. There is no evidence of a second threshold above 2.0 MeV in the excitation function measurement; therefore, we cannot attribute the  $\gamma$  ray to the higher 2219.35-keV level.

**1978.42- and 2219.35-keV levels:  $3^+$  and  $4^+$**

The current experiments confirm the assignment of the 350.05-keV  $\gamma$  ray to the level at 1978.42 keV. In  $^{96}\text{Nb}$  decay, Monaro *et al.* [35] found a triplet and Taylor *et al.* [33] found

TABLE II. Transition probabilities calculated for the positive parity states with short lifetimes. When two  $\delta$  values are possible, the one with the lower  $\chi^2$  is used. If they are equally likely, values for both are calculated. Limiting values of zero and infinity are assumed for rates presented.

$E_L$ (keV)	$J_i^\pi$	$E_f$ (keV)	$J_f^\pi$	$B(E1)$ ( $\times 10^{-3}$ W.u.)	$B(M1)$ ( $\mu_N^2$ )	$B(E2)$ (W.u.)	Notes
778.22	$2_1^+$	0.00	$0_g^+$			20.7(3)	a
1148.12	$0_2^+$	778.22	$2_1^+$			74(10)	a
1497.76	$2_2^+$	778.22	$2_1^+$		0.05(3)	59(36)	
					$0.09^{+0.09}_{-0.06}$	$11^{+12}_{-7}$	
		0.00	$0_g^+$			$1.1^{+0.7}_{-0.6}$	
1625.88	$2_3^+$	778.22	$2_1^+$		<0.05	<45	
					<0.005	<160	
		0.00	$0_g^+$			<4	
1628.20	$4_1^+$	778.22	$2_1^+$			$59^{+12}_{-8}$	a
1869.53	$4_2^+$	1628.20	$4_1^+$		0.05(2)	$12^{+5}_{-4}$	a
					$0.015^{+0.008}_{-0.006}$	$330^{+178}_{-132}$	
		778.22	$2_1^+$			3(1)	
1978.42	$3_1^+$	1628.20	$4_1^+$		<0.034	<0.24	
					<0.001	<150	
		1625.88	$2_3^+$		<0.010	<10	
					<0.0007	<50	
		1497.76	$2_2^+$		<0.04	<1.4	
		778.2	$2_1^+$			<2.4	
2095.73	$2_{ms}^+$	778.22	$2_1^+$		0.17(2)	$0.44^{+0.06}_{-0.05}$	
		0.00	$0_g^+$			$0.08^{+0.02}_{-0.01}$	
2234.63	$3_1^-$	1869.53	$4_2^+$	<1.0			
		1625.88	$2_3^+$	<2.4			
		1497.76	$2_2^+$	<1.3			
		778.22	$2_1^+$	<0.02			
2426.07	$2_5^+$	1978.42	$3_1^+$		$0.008^{+0.008}_{-0.004}$	$140^{+90}_{-110}$	
		1625.88	$2_3^+$		$0.14^{+0.04}_{-0.03}$	$4.0^{+1.0}_{-0.8}$	
		1497.76	$2_2^+$		0.0006(4)	$6.2^{+5.7}_{-2.7}$	
		778.22	$2_1^+$		$0.010^{+0.004}_{-0.003}$	$3.0^{+1.3}_{-1.0}$	
		0.00	$0_g^+$			$0.07^{+0.02}_{-0.01}$	
2625.23	$4_5^+$	2219.35	$4_3^+$		$0.18^{+0.14}_{-0.12}$	$82^{+63}_{-53}$	
					$0.03^{+0.04}_{-0.03}$	$579^{+1082}_{-447}$	
		778.22	$2_1^+$			$1.8^{+1.2}_{-1.1}$	
2700.08	$2_6^+$	1497.76	$2_2^+$		$0.10^{+0.02}_{-0.01}$	$0.48^{+0.08}_{-0.06}$	b
					[ $0.009^{+0.004}_{-0.003}$ ]	[ $36^{+15}_{-12}$ ]	
		778.22	$2_1^+$		0.019(3)	$0.15^{+0.03}_{-0.02}$	
					0.007(2)	$2.0^{+0.6}_{-0.5}$	
		0.00	$0_g^+$			$0.22^{+0.05}_{-0.04}$	
2735.98	$3_3^+$	1497.76	$2_2^+$		0.06(1)	2.3(4)	
		778.22	$2_1^+$		$0.028^{+0.003}_{-0.002}$	$0.0016^{+0.0003}_{-0.0002}$	
2787.07	$2_7^+$	1625.88	$2_3^+$		$0.007^{+0.002}_{-0.001}$	$0.46^{+0.15}_{-0.21}$	
		1497.76	$2_2^+$		$0.004^{+0.004}_{-0.003}$	$1.8^{+1.7}_{-1.4}$	
		778.22	$2_1^+$		$0.028^{+0.004}_{-0.006}$	$0.22^{+0.03}_{-0.05}$	
					0.0005(3)	$3.9^{+3.0}_{-1.8}$	
2794.34	$1_1^+$	1497.76	$2_2^+$		0.11(2)	$36^{+7}_{-6}$	c
		778.22	$2_1^+$		0.018(3)	$2.4^{+0.5}_{-0.4}$	c
		0.00	$0_g^+$		$0.040^{+0.006}_{-0.005}$		
2818.53	$4_7^+$	1628.20	$4_1^+$		$0.39^{+0.10}_{-0.09}$	$3.0^{+0.8}_{-0.7}$	



TABLE II. (Continued.)

$E_L$ (keV)	$J_i^\pi$	$E_f$ (keV)	$J_f^\pi$	$B(E1)$ ( $\times 10^{-3}$ W.u.)	$B(M1)$ ( $\mu_N^2$ )	$B(E2)$ (W.u.)	Notes
2986.79	$2_8^+$	2095.73	$2_{\text{ms}}^+$		0.09(2)	$4.4^{+0.9}_{-0.7}$	
		1978.42	$3_1^+$		$0.034^{+0.008}_{-0.007}$	1.8(4)	
					0.004(4)	$18^{+31}_{-10}$	
		1625.88	$2_3^+$		$0.033^{+0.008}_{-0.007}$	$4.6^{+1.2}_{-0.94}$	
		778.22	$2_1^+$		0.002(1)	$14^{+11}_{-5}$	
		0.00	$0_g^+$		$0.009^{+0.002}_{-0.001}$	$0.003^{+0.005}_{-0.004}$	
					0.0006 $^{+0.0005}_{-0.0004}$	$1.0^{+0.9}_{-0.7}$	
3006.42	$0_3^+$	1497.76	$2_2^+$			$0.11^{+0.03}_{-0.02}$	
3024.47	$2_9^+$	1978.42	$3_1^+$		$0.06^{+0.02}_{-0.01}$	$31^{+6}_{-5}$	
					0.014(3)	3.2(8)	
		1869.53	$4_2^+$			$27^{+7}_{-5}$	
		1628.20	$4_1^+$			11(2)	
		1625.88	$2_3^+$			$21^{+4}_{-3}$	
3087.70	$3_4^+$	2095.73	$2_{\text{ms}}^+$		$0.045^{+0.001}_{-0.008}$	$2.9^{+0.7}_{-0.6}$	
		1628.20	$4_2^+$		$0.025^{+0.020}_{-0.016}$	$0.17^{+0.14}_{-0.10}$	
					$0.006^{+0.005}_{-0.005}$	$2.8^{+2.7}_{-1.9}$	
		1625.88	$2_3^+$		$0.013^{+0.010}_{-0.008}$	$0.9^{+0.7}_{-0.6}$	
3178.74	$3_2^-$	2234.63	$3_1^-$		$0.0014^{+0.0018}_{-0.0011}$	$3.1^{+3.9}_{-2.3}$	
		2095.73	$2_{\text{ms}}^+$	$0.09^{+0.03}_{-0.02}$	0.04(1)	$2.4^{+0.03}_{-0.02}$	
		1497.76	$2_2^+$	$0.08^{+0.02}_{-0.01}$			
		778.22	$2_1^+$	0.11(2)			
3211.35	$3_5^+$	1978.42	$3_1^+$		0.009(5)	$20^{+16}_{-8}$	
					0.06(2)	$1.1^{+0.03}_{-0.02}$	
		1869.53	$4_2^+$		$0.001^{+0.011}_{-0.008}$	$10^{+10}_{-8}$	
		1497.76	$2_2^+$		$0.0007^{+0.008}_{-0.003}$	$4^{+2}_{-3}$	
		778.22	$2_1^+$		$0.004^{+0.001}_{-0.008}$	$1.4^{+0.4}_{-0.3}$	
3284.89	$2_{11}^+$	778.22	$2_1^+$		$0.00014^{+0.00011}_{-0.00016}$	$0.37^{+0.64}_{-0.22}$	
					$0.006^{+0.010}_{-0.003}$	$1.2^{+0.9}_{-0.2}$	
3300.56	$1_2^+$	1497.76	$2_2^+$		$0.07^{+0.03}_{-0.02}$	$12^{+5}_{-3}$	c
		0.00	$0_g^+$		$0.12^{+0.03}_{-0.02}$		
3352.01	$2_{12}^+$	2095.73	$2_{\text{ms}}^+$		$0.20^{+0.08}_{-0.05}$	$0.69^{+0.26}_{-0.19}$	
		1497.76	$2_2^+$		$0.019^{+0.019}_{-0.008}$	7(4)	
		0.00	$0_g^+$			$0.38^{+0.14}_{-0.11}$	
3374.09	$2_{13}^+$	1625.88	$2_3^+$		$0.007^{+0.005}_{-0.008}$	$15^{+21}_{-8}$	
					$0.09^{+0.02}_{-0.01}$	0.23(4)	
		778.22	$2_1^+$		0.06(1)	1.2(2)	
3424.86	$1_3^+$	778.22	$2_1^+$		0.02(1)	$1.4^{+0.9}_{-0.6}$	c
		0.00	$0_g^+$		$0.11^{+0.04}_{-0.03}$		
3433.58	$4_8^+$	778.22	$2_1^+$			$1.7^{+0.04}_{-0.03}$	
3441.97	$4_9^+$	778.22	$2_1^+$			$0.94^{+0.028}_{-0.025}$	
3599.56	$1^-$	778.22	$2_1^+$	$0.30^{+0.18}_{-0.12}$			
		0.00	$0_g^+$	$0.52^{+0.17}_{-0.11}$			
3668.51	$3_6^+$	1628.20	$4_1^+$		$0.003^{+0.008}_{+0.002}$	$6^{+5}_{-10}$	
		778.22	$2_1^+$		$0.016^{+0.005}_{-0.003}$	$0.21^{+0.06}_{-0.05}$	
					$0.008^{+0.004}_{-0.006}$	$0.74^{+0.75}_{-0.30}$	

<sup>a</sup>Value taken from Ref. [32].

<sup>b</sup>Transition probabilities are upper limits, since additional  $\gamma$ -ray branches could be obscured by background lines.

<sup>c</sup>No  $\delta$  values were obtained from our data.

a doublet with  $\gamma$ -ray energies 350.0 and 350.7 keV. The  $(n, \gamma)$  experiment placed a 349.7-keV  $\gamma$  ray from either the 1978- or 2219-keV level [17]. We were only able to observe a 350.05-keV  $\gamma$  ray and saw no evidence of the  $\gamma$  ray being a doublet. From our excitation function, we were able to determine the  $\gamma$ -ray thresholds; in particular, the 350.05-keV  $\gamma$  ray belongs to the level at 1978.42 keV.

#### 2095.73-keV level: $2^+$

A  $\gamma$  ray at 947.8 keV was assigned to this level in  $(n, \gamma)$  work [17]. From the excitation function, we were able to verify that the  $\gamma$  ray is produced with 2.0 MeV neutrons. Clearly, this transition cannot deexcite the 2095.73-keV level. An investigation into the identity of this  $\gamma$  ray exposed a strong transition at this energy in  $^{95}\text{Mo}$ , which might account for its accidental attribution to  $^{96}\text{Mo}$ . There are actually only two  $\gamma$ -ray decays associated with this level, to the  $2_1^+$  level and the ground state. The MS properties of this level will be further discussed in Sec. VI.

#### 2481.04-keV level: $4^+$

In a  $(p, p')$  experiment, Fretwurst *et al.* [21] assigned a spin-parity of  $4^+$  to this level; however, in the Nuclear Data Sheets (NDS), a spin was not adopted [32]. The two  $\gamma$  rays observed in this experiment and the STAT-MOD calculations for the level excitation function support a  $J = 4$  spin assignment. This is most likely the  $L = 4$  excitation observed at  $2476 \pm 8$  keV in  $(t, p)$  [36] and  $(\alpha, \alpha')$  [20] reaction studies.

#### 2501.50-keV level: $1$

The spin of this level had been tentatively assigned in NDS as  $J = 1$  [32]. Both our data and a previous measurement support this assignment [37]. In addition, we have assigned two  $\gamma$ -ray decays, to the  $0_6^+$  and  $2_3^+$  states, and determined a lifetime of  $\tau = 140 \pm 19$  fs. A  $\gamma$  ray with an energy of  $2502.2 \pm 1.5$  keV was observed in the  $(n, \gamma)$  reaction [17], but remained unassigned. We believe this is the same ground-state transition we observed for this level at 2501.84(8) keV. We were unable to assign the parity.

#### 2540.34-keV level: ( $2^+, 3^+$ )

A 914.6-keV  $\gamma$  ray was previously assigned to both the 2540- and 3134-keV levels [17]. From our excitation function, the placement to the 2540.34-keV level is confirmed. This work equally supports  $J^\pi = 2^+$  or  $3^+$ .

#### 2594.34-keV level: $3^+$

An 1815.4-keV  $\gamma$  ray had been assigned to levels at 2594 and 3442 keV in an  $(n, \gamma)$  measurement [17]. From our excitation function threshold, we were able to confirm the assignment to the former level, agreeing with the assignment in Ref. [19]. The 1096.62-keV transition was observed, but we were unable to obtain an intensity, because this  $\gamma$  ray is in the same energy region as a laboratory background line. For

the same reason, lifetime measurements and branching ratios were unreliable and therefore not reported. A previous  $^{96}\text{Nb}$  decay experiment assigned a tentative spin of  $J^\pi = 4^+$  but was unable to rule out a  $3^+$  assignment [35]. An angular distribution and STAT-MOD calculations for the  $\gamma$  ray observed at 968.54 keV give only one possibility,  $J = 3$ . The calculation gives two equally probable  $\delta$  values, neither of which can be zero; therefore,  $J^\pi = 3^+$  is a definite assignment.

#### 2622.48- and 2625.23-keV levels: $0^+$ and $4^+$

A level was identified at 2622.48 keV from an 1844.25-keV  $\gamma$  ray to the  $2_1^+$  level, yielding a lifetime of  $\tau = 840_{-300}^{+870}$  fs. We find a close-lying level at 2625.23 keV, which decays via an 1846.98-keV  $\gamma$  ray. The excitation functions of these  $\gamma$  rays exhibit different neutron energy dependencies, clearly indicating that they have different spins. In  $(t, p)$  data, a level at  $2621 \pm 10$  keV is given and assigned a spin of  $4^+$  [36]. It is uncertain which level the transfer experiment observed, since the large energy uncertainty would encompass both levels. We leave the 2625.23-keV level assignment unchanged. Spin 0 is assigned to the 2622.48-keV level from the excitation function of that level.

#### 2700.08-keV level: $2^+$

Although this level was observed from deexciting  $\gamma$  rays in a previous experiment [17], no spin assignment was made. The angular distributions permitted a spin of 2 or 3. With our identification of a new quadrupole transition to the ground state,  $a_2 = 0.32 \pm 0.05$  and  $a_4 = -0.04 \pm 0.07$ , we were able to exclude the  $J = 3$  possibility and could definitely assign a spin of  $2^+$ . The STAT-MOD-calculated excitation function also supports this assignment.

#### 2735.98-keV level: $3^+$

Information obtained from previous measurements gives the 2735.98-keV level a possible  $J^\pi = (3^+, 4^+)$  spin assignment [18]. We were able to assign a previously observed but unplaced [17]  $\gamma$  ray, 1238.17 keV, to this level; and from angular distributions and the level excitation function, we were able to support only a  $J^\pi = 3^+$  assignment.

#### 2749.71-keV level: $0^+$

A  $(p, t)$  experiment excited a level at  $\sim 2750$  keV, based on the traditional strong peak angular distribution which usually signals unambiguously an  $\ell = 0$  transfer to a  $0^+$  excited level [22]. However, a weak line at that energy was detected in a photon scattering experiment [37] which would require a  $J = (1, 2)$ . The photon scattering experiment did not observe excited level decays from the excitation and thus found that the ground-state transition intensity strongly dominated the level's decay.

Present measurements, however, show the decay of the 2749.71-keV level to be entirely due to two decays to excited levels, with no observable ground-state transitions. Hence this level fits well as a  $0^+$  level in the STAT-MOD calculations and

does not correspond to the photon scattering peak. Therefore, the level is firmly assigned as a  $0^+$ .

#### 2790.24-keV level: $2, 4$

The spin for this level remains unassigned in NDS; but  $6^+$  is assigned to a 2791.4-keV level in Ref. [38]. We were not able to support the  $6^+$  assignment but instead we assign a spin of  $J = 2$  or  $4$  from the angular distributions of  $\gamma$  rays to  $2^+$  and  $3^-$  levels. In addition, we place a  $\gamma$  ray of 1292.99 keV from this level. Although we were able to deduce the existence of the transition, we were unable to obtain an accurate lifetime, branching ratio, or multipole mixing ratio, since this  $\gamma$  ray is contaminated by a background  $\gamma$  ray.

#### 2794.34-keV level: $1^+$

This level was identified at 2794.5 keV and assigned a spin of  $J = 1$  [37]. From a more recent measurement with polarized photons [25], the ground-state decay was found to be an  $M1$  transition, and therefore  $J^\pi = 1^+$  is firmly assigned. Our angular distribution data support this finding with  $a_2 = -0.19 \pm 0.03$  and  $a_4 = 0.04 \pm 0.35$  for the ground-state transition. The possible MS properties of this level will be discussed in Sec. VI.

#### 2806.23-keV level: $1$

From  $(p, p')$  data, this level was assigned  $J^\pi = (3^-)$  [21] and from  $(\gamma, \gamma')$ ,  $J = 1$  [37]. We have placed two new  $\gamma$  rays at 1180.42 and 1658.10 keV from this level to the  $2_3^+$  and  $0_2^+$  levels, respectively. Since we observe decay to the  $0_2^+$  state with small anisotropy, this level cannot be  $J^\pi = 3^-$ ; therefore, we support the  $J = 1$  spin assignment. A 1657.6-keV  $\gamma$  ray was reported in an  $(n, \gamma)$  experiment and assigned to a level at 3284 keV [17], listed in Table I as 1658.10 keV. Our excitation function data excludes this possibility and places it with the current level.

#### 2975.41-keV level: $4$

A previous  $(n, \gamma)$  experiment assigned a 740.7-keV  $\gamma$  ray to levels at 2975 and 3335 keV [17]. From the excitation function, we were able to confirm the assignment of a 740.59-keV  $\gamma$  ray to the 2975.41-keV level. The spin was assigned as  $J^\pi = (5^+, 6^+)$  in Ref. [18]. The angular distribution of the 740.59-keV  $\gamma$  ray only allows  $J = 2, 4$ , while the 1347.26-keV  $\gamma$  ray allows  $J = 3-6$ . Since both  $\gamma$  rays are from the same level, the only possible value is  $J = 4$ .

#### 2986.79-keV level: $2^+$

Our data confirm the  $J^\pi = 2^+$  assignment given in the NDS compilation [32] with a newly observed  $E2$  ground-state transition, which has an angular distribution fit with  $a_2 = 0.26 \pm 0.08$  and  $a_4 = 0.06 \pm 0.12$ . The lifetime has been

determined from our measurements to be  $\tau = 150_{-20}^{+21}$  fs. This state will be discussed later in Sec. VI.

#### 3006.42-keV level: $0^+$

The 1508.65-keV  $\gamma$  ray was assigned to the 3134.50-keV level in  $(n, \gamma)$  work from energy considerations [17]. From the shape of the cross section, the  $\gamma$  ray may belong to the 3134.50-keV level, but the rise of the excitation function is steeper than the excitations known to be from this level. This observation leads us to believe it may be a  $3006.42 \rightarrow 1497.76$ -keV transition. Because of this uncertainty, the  $\gamma$  ray is placed twice in the level scheme.

#### 3087.70-keV level: $3^+$

A spin of  $J^\pi = (4^-, 5^-)$  was assigned to this level in  $(p, p')$  measurements [21]. Our angular distribution data for the three deexciting  $\gamma$  rays only allows for one spin assignment,  $J = 3$ . In view of the nonzero mixing ratio determined for one transition, the assignment must be  $3^+$ .

#### 3089.65-keV level: $2, 3$

A newly discovered level at 3089.65 keV is assigned using two  $\gamma$  rays to  $2_1^+$  and  $2_2^+$  states. The 1591.89-keV  $\gamma$  ray had been seen in a  $(n, \gamma)$  experiment, but remained unassigned [17]. The other, 2311.29 keV, is a new observation of this work and is placed by our excitation function. A lifetime of  $\tau = 95_{-12}^{+14}$  fs has been determined. The spin is limited to  $J = 2, 3$  from the angular distributions.

#### 3134.50-keV level: $2^+$

This level was identified in  $(n, \gamma)$  [17] measurements by a deexciting  $\gamma$ -ray decay, although no spin assignment was made. A new ground-state transition has been observed, with a positive  $a_2 = 0.29 \pm 0.04$  and a negative  $a_4 = -0.02 \pm 0.06$ , which is indicative of a quadrupole transition; therefore,  $2^+$  is assigned to this level. The  $\gamma$  ray at 1508.65 keV had been placed by energy considerations in Ref. [17]. The neutron energy dependence of the excitation function is compared with that of other  $\gamma$  rays from this level, and the similarity makes this assignment possible, within uncertainties. A  $\gamma$  ray of essentially the same energy is placed from the level at 3006.42 keV, noted above.

#### 3154.13-keV level: $1$

Another new discovery is the level assigned from observation of a  $\gamma$  ray to the first  $2^+$  state. This  $\gamma$  ray was observed in  $(n, \gamma)$  work, but left unassigned [17]. A spin of  $J = 1$  is indicated by the STAT-MOD excitation function calculations.

#### 3178.74-keV level: $3^-$

A spin of  $J^\pi = 3^-$  was assigned in Refs. [20,32] to a level with energy of 3.17 MeV, but  $4^+$  was adopted in NDS [32]. The present data support a spin of  $J = 3$ , and excludes  $J = 4$ , for

this level from STAT-MOD angular distribution calculations. Two previously observed but unassigned  $\gamma$  rays with energies of 944.10 [17] and 1680.87 keV [32] are placed from this level.

### 3232.45-keV level: 3

This newly established level is placed by  $\gamma$ -ray decays to the  $2_1^+$  and  $2_3^+$  levels. Although the excitation function of this level's decay seems characteristic of a  $J = 4$  level, the STAT-MOD-calculated angular distribution could only represent a transition from a  $J = 3$  level. Missing weak lines from the level would account for the lack of yield in the excitation function. The parity could not be determined.

### 3300.56-keV level: $1^+$

The second  $1^+$  state is at 3300.56 keV, with spin and parity identifications as described for the 2794.34-keV level [25,37]. Our data support this assignment with angular distribution coefficients  $a_2 = -0.22 \pm 0.15$  and  $a_4 = 0.02 \pm 0.21$  for the ground-state transition. A  $B(M1)$  to the ground state of  $0.12_{-0.02}^{+0.03} \mu_N^2$  and  $B(M1; 1_2^+ \rightarrow 2_2^+) = 0.07_{-0.02}^{+0.03} \mu_N^2$  were also obtained.

### 3352.01-keV level: $2^+$

This level was identified in Ref. [37] at an energy of 3352.3 keV and assigned a spin of  $J = 1$ . In our measurement, we found  $\gamma$ -ray decays from this level at 1255.75, 1854.35, and 3351.04 keV. From the ground-state transition, we see a large, positive  $a_2$  value ( $0.69 \pm 0.19$ ) and small  $a_4$  value ( $0.26 \pm 0.28$ ), indicating a characteristic of a quadrupole,  $E2$  decay. The other two  $\gamma$  rays are fit with theoretical calculations which also support  $J = 2$ ; therefore, we adopt  $J^\pi = 2^+$  for this level.

### 3416.82-keV-level: $4^+$

Two  $\gamma$ -ray transitions from this level were identified in a  $(n, \gamma)$  study, and the level was assigned in that work [17]. The 1320.9-keV  $\gamma$  rays, presumed to be a doublet, were placed from both the 2819 and 3417 levels. From our excitation function, we were able to place only one transition from the 3416.82-keV level. A 2639.7-keV  $\gamma$  ray was observed but remained unassigned in the  $(n, \gamma)$  work [17], listed as 2638.55 keV in Table I. We are also able to assign this  $\gamma$ -ray transition to the current level through the excitation function and angular distribution, which has the stretched  $E2$  character expected of a  $4^+$  to  $2^+$  transition.

### 3668.51-keV level: $3^+$

There are two  $\gamma$ -ray decays from the new level at 3668.51 keV: a 2890.16-keV transition to the  $2_1^+$  level and a 2041.36-keV  $\gamma$  ray to the  $4_1^+$  level. The STAT-MOD calculations for the  $\gamma$  ray to the  $2_1^+$  level gives only one possible

spin,  $J = 3$ . There are two equally probable  $\delta$  values, neither of which can be zero, yielding a positive parity assignment.

## V. MULTIPHONON SYMMETRIC STATES

In the geometric vibrational model [39], two-phonon states should lie at approximately twice the energy of the one-phonon state and are expected to have a  $B(E2)$  ratio of  $\frac{B(E2; J_i^\pi \rightarrow 2_1^+)}{B(E2; 2_1^+ \rightarrow 0_g^+)} = 2$ . The  $B(E2; 2_1^+ \rightarrow 0_g^+)$  in  $^{96}\text{Mo}$  is 20.7(3) W.u., and the transition from the  $2^+$  level at 1497.76 keV has a  $B(E2)$  value of 59(36) W.u., giving a ratio of about 3, but with large uncertainty. Only a limit for the lifetime of the  $2_3^+$  level at 1625.88 keV was measured, but since the  $2_2^+$  and  $2_3^+$  states lie at similar excitation energies and have similar decay properties, it may be that both states contribute to the two-phonon strength in  $^{96}\text{Mo}$ . Also, although the energy for the the first  $0^+$  excited state is rather low, at 1148.12 keV, and its determined lifetime [32] is beyond the range of the present measurements, the extremely large  $B(E2)$  value of 74(10) W.u. may still indicate two-phonon character. The  $4^+$  state at 1628.20 keV fits reasonable well in both energy,  $E(4^+)/E(2_1^+) = 2.09$ , and as the  $B(E2)$  ratio  $\frac{B(E2; 4_1^+ \rightarrow 2_1^+)}{B(E2; 2_1^+ \rightarrow 0_g^+)} = \frac{59_{-3}^{+12}}{20.7(3)} \frac{\text{W.u.}}{\text{W.u.}} > 2$ . So, although the  $M1$  transitions discussed in the mixed-symmetry section suggest that  $^{96}\text{Mo}$  is closer to O(6) symmetry than U(5), the vibrational picture may remain partially intact through the one- and two-phonon structures.

## VI. MIXED-SYMMETRY STATES

Although  $^{96}\text{Mo}$  has been treated at low energies as a vibrator, it is expected to be transitional between vibratorlike nuclei and deformed rotors. For deformed rotational nuclei, the  $M1$  transition from the  $1_{sc}^+$  level to the ground state is the dominant mixed-symmetry transition. But for  $\gamma$ -soft or vibrational nuclei, the dominant  $M1$  transition is from the  $2_{ms}^+$  state to the  $2_1^+$  level, the first excited state.

### A. The $2_{ms}^+$ state

The search for the  $2_{ms}^+$  state, the fundamental one-phonon MS excitation, began with an examination of the  $B(M1)$  values of decays from the  $2^+$  states below 3 MeV to the first excited level [9]. These results are shown in Table III, where the fourth

TABLE III. Comparison of  $M1$  transition rates from decays of  $2^+$  states in  $^{96}\text{Mo}$  to the first excited  $2^+$  state ( $2_1^+$ ).

$E_L$ (keV)	$J_i^\pi$	$E_\gamma$ (keV)	$B(M1)(\mu_N^2)$
1625.88	$2_3^+$	847.67	<0.05
2095.73	$2_4^+$	1317.50	0.17(2)
2426.07	$2_5^+$	1647.82	$0.010_{-0.003}^{+0.004}$
2700.08	$2_6^+$	1921.78	0.019(3)
2787.07	$2_7^+$	2008.82	$0.028_{-0.006}^{+0.004}$
2986.79	$2_8^+$	2208.55	$0.009_{-0.001}^{+0.002}$

$2^+$  state ( $2_4^+$ ), at 2095.73 keV clearly exhibits the largest  $B(M1)$  value. From the lifetime of  $\tau = 140 \pm 16$  fs and multipole mixing ratio of  $\delta = -0.09(2)$ , a  $B(M1; 2_4^+ \rightarrow 2_1^+)$  of  $0.17(2) \mu_N^2$  was determined. The reduced matrix element,  $|\langle 2_1^+ || M1 || 2_4^+ \rangle| = 0.94 \mu_N$ , is in keeping with that expected for a mixed-symmetry state. This state appears to be the principal component of the fundamental MS excitation.

The  $2_{\text{ms}}^+$  states in other nuclei in this region including  $^{94}\text{Mo}$  and  $^{96}\text{Ru}$  also occur near 2 MeV. The ground-state  $E2$  transitions have  $B(E2; 2_{\text{ms}}^+ \rightarrow 0_g^+)$  values in  $^{94}\text{Mo}$  of 2.2 W.u. [4], in  $^{92}\text{Zr}$  [13] of 3.4 W.u., and in  $^{96}\text{Ru}$  of 1.6 W.u. [14]. The  $^{96}\text{Mo}$  nucleus exhibits a much lower value of 0.08 W.u. The  $B(M1; 2_{\text{ms}}^+ \rightarrow 2_1^+)$  values of the different nuclei vary, with the current study for  $^{96}\text{Mo}$  producing the lowest value. This value, while lower than that of neighboring nuclei, is quite appropriate for a mixed-symmetry excitation.

With the lowest MS state in  $^{96}\text{Mo}$  identified, two-phonon states can be sought. The  $2_1^+ \otimes 2_{\text{ms}}^+$  coupling should lead to a quintuplet of states around 2.9 MeV, the sum energy of these states,  $E(2_1^+) + E(2_{\text{ms}}^+)$ .

### B. Two-phonon $1^+$ MS state

Levels at 2794.5 and 3300.1 keV were identified in nuclear resonance fluorescence (NRF) measurements [37] and assigned  $J = 1$ . Our angular distribution data provide agreement with those assignments. From a more recent measurement with polarized photons [25], the ground-state transitions from these levels were determined to be  $M1$  in character, and therefore  $J^\pi = 1^+$  is firmly assigned. We observed the ground-state transitions and those to the  $2_2^+$  state from both levels as shown in Table I. The 2794.34-keV ground-state transition has a  $B(M1; 1_1^+ \rightarrow 0_g^+)$  of  $0.040_{-0.005}^{+0.006} \mu_N^2$ , appropriately weak for a cross-over, two-phonon transition. We were unable to obtain a multipole mixing ratio for the weak  $1_1^+ \rightarrow 2_2^+$  transition. If we assume pure  $M1$  character for this transition, we determine an  $M1$  transition strength of  $B(M1; 1_1^+ \rightarrow 2_2^+) = 0.11(2) \mu_N^2$ , which is strong enough to suggest MS character. On the other hand, for the assumption of a pure  $E2$  transition, we determine  $B(E2; 1_1^+ \rightarrow 2_2^+) = 36_{-6}^{+7}$  W.u., which seems be unrealistically large.

The other  $1^+$  level, at 3300.56 keV, has a stronger ground-state transition,  $B(M1; 1_2^+ \rightarrow 0_g^+) = 0.12_{-0.02}^{+0.03} \mu_N^2$ , but about 60% of the transition strength to the  $2_2^+$  state,  $B(M1; 1_2^+ \rightarrow 2_2^+) = 0.07_{-0.02}^{+0.03} \mu_N^2$ . The  $M1$  transition probability of the  $1_2^+ \rightarrow 2_2^+$  transition is small and is the maximum value permitted, based on our data, since the  $\delta$  value could not be obtained for the 1802.81-keV  $\gamma$  ray.

Another level, at 3424.86 keV, with spin and parity  $1^+$  ( $1_3^+$ ), has been firmly assigned by NRF and polarized photon methods [25,37]. Only two  $\gamma$ -ray transitions were identified: to the ground state,  $B(M1; 1_3^+ \rightarrow 0_g^+) = 0.11_{-0.03}^{+0.04} \mu_N^2$ , and to the  $2_1^+$  state,  $B(E2; 1_3^+ \rightarrow 2_1^+) = 1.4_{-0.6}^{+0.9}$  W.u. with a small  $B(M1; 1_3^+ \rightarrow 2_1^+) = 0.02(1) \mu_N^2$  component. If this level is dominantly an  $E2$  transition, it is only  $\sim 1.4$  W.u.; and if a pure  $M1$ , the strength is low, therefore this level is not a

collective excitation. No decay was observed to the  $2_{\text{ms}}^+$  state or any two-phonon symmetric state. The decay pattern and collectivity are inconsistent with transitions expected from mixed-symmetry states. The absence of the main signatures prevents the level at 3424.86 keV from being considered as a MS state.

The  $M1$  transition probabilities of decays from the  $1^+$  states in  $^{96}\text{Mo}$  and, for comparison,  $^{94}\text{Mo}$  to the ground state and  $2_2^+$  state are summarized in Fig. 6. The expected signatures of the  $1_{\text{ms}}^+$  states are strong  $M1$  transitions principally to the  $2_2^+$  levels; but for those nuclei tending toward  $O(6)$  symmetry, transitions can be observed they are also to the ground states. From this figure, fragmentation of the  $^{96}\text{Mo}$  MS strength between the known  $1^+$  levels at 2794.34 and 3300.56 keV is evident, similar to the  $^{94}\text{Mo}$   $1^+$  mixed-symmetry states.

### C. Two-phonon $2^+$ MS state

There are two possibilities for the two-phonon MS  $2^+$  state (denoted  $2_{2,\text{ms}}^+$ ): the states observed at 2700.08 and 2986.79 keV. For identification of the  $2_{2,\text{ms}}^+$  state, two transitions were of particular interest. First was the decay to the symmetric  $2_2^+$  state at 1497.76 keV. For the 2700.08-keV level, an  $E2/M1$  mixing ratio of  $\delta = -0.11(5)$  was determined, with a corresponding  $B(M1; 2_6^+ \rightarrow 2_2^+) = 0.10_{-0.01}^{+0.02} \mu_N^2$  and small  $B(E2; 2_6^+ \rightarrow 2_2^+) = 0.48_{-0.06}^{+0.08}$  W.u. This multipole mixing ratio fits the angular distribution for the 1202.43-keV

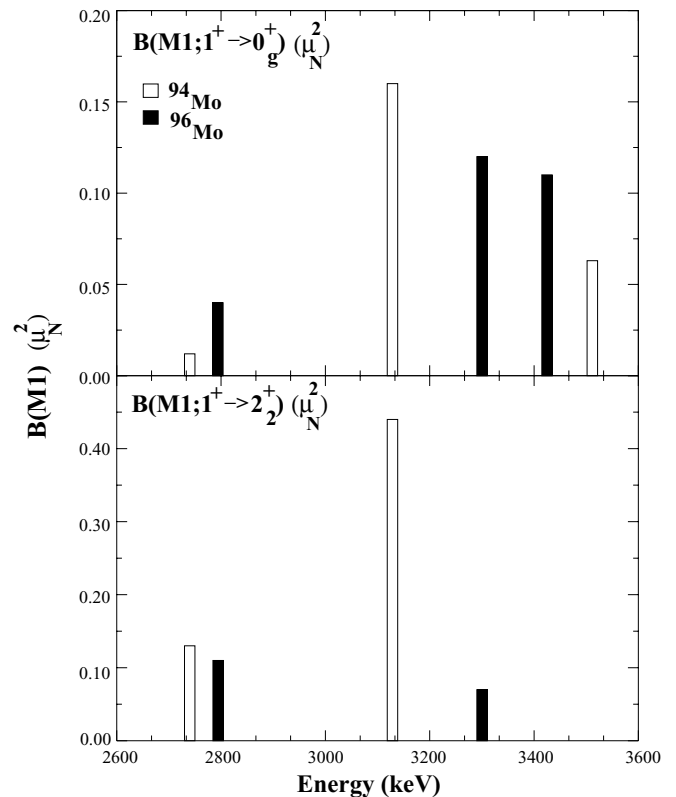


FIG. 6. Comparison of  $M1$  transition rates of  $1^+$  strength in  $^{94}\text{Mo}$  [6] and  $^{96}\text{Mo}$ .

transition with the smallest  $\chi^2$  and is thus the best fit in contrast to an alternative fit with a  $\delta = 3.3(6)$  value. Therefore, the smaller value of  $\delta$  was adopted. The resulting  $B(M1)$  value is greater than that from any other  $2^+$  state in the energy region. The ground-state transition has a small  $B(E2; 2_6^+ \rightarrow 0_g^+)$  of  $0.22_{-0.04}^{+0.05}$  W.u. These values are consistent with those expected of the  $2_{2,\text{ms}}^+$  state.

A possible fragment of the  $2_{2,\text{ms}}^+$  excitation is the 2986.79-keV level, which has two signatures expected of such an excitation. It has a strong decay to the fundamental MS state and a weak  $E2$  to the ground state,  $B(E2) = 0.11_{-0.02}^{+0.03}$  W.u. There is also a weak transition to the  $2_1^+$  level,  $B(E2) = 0.003_{-0.004}^{+0.005}$  W.u., as would be expected of a two-phonon level. But we have identified no  $M1$  transition to the  $2_2^+$  level. Strong  $M1$  transitions to the appropriate fully symmetric levels are the primary signatures of MS excitations. Therefore, we conclude that the 2700.08-keV level is the primary  $2_{2,\text{ms}}^+$  excitation.

#### D. Two-phonon $3^+$ MS state

We have also identified a candidate for the two-phonon  $3_{\text{ms}}^+$  state at 2735.98 keV and obtain  $B(M1; 3^+ \rightarrow 2_2^+) = 0.06(1) \mu_N^2$ , with a small  $E2$  contribution of 2.3(4) W.u. Another signature is the decay to the  $2_1^+$  state, which is seen here with  $B(E2; 3^+ \rightarrow 2_1^+) = 0.028_{-0.002}^{+0.003}$  W.u. From these transition probabilities, this level represents the best candidate for the  $3_{\text{ms}}^+$  state to date.

#### E. Comparison and calculations

These assignments in  $^{96}\text{Mo}$  can be compared with those in the well-known  $^{94}\text{Mo}$  nucleus. Figures 6 and 7 give comparisons for the  $1^+$  MS states. There is a noticeable difference in  $B(M1)$  strength distributions between the two nuclei. The  $M1$  transition from the main fragment of the two-phonon MS  $1^+$  state in  $^{94}\text{Mo}$  to the symmetric two-phonon

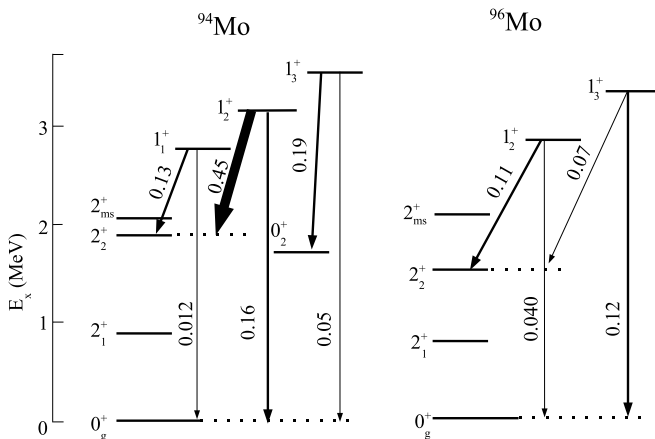


FIG. 7. Comparison of decays of  $1^+$  states contributing to the  $1_{\text{ms}}^+$  state in  $^{94}\text{Mo}$  [6] and  $^{96}\text{Mo}$  (current work).  $B(M1)$  values are given in  $\mu_N^2$ .

TABLE IV. Comparison between the  $B(M1)$  values from Ref. [25] and the current data.

Observable	Ref. [25]	Expt.
$B(M1; 1_1^+ \rightarrow 0_g^+)$	0.024(3)	$0.040_{-0.005}^{+0.006}$
$B(M1; 1_1^+ \rightarrow 2_2^+)$	–	0.11(2)
$B(M1; 1_2^+ \rightarrow 0_g^+)$	0.051(3)	$0.12_{-0.02}^{+0.03}$
$B(M1; 1_2^+ \rightarrow 2_2^+)$	–	$0.07_{-0.02}^{+0.03}$
$B(M1; 1_3^+ \rightarrow 0_g^+)$	0.081(3)	$0.11_{-0.03}^{+0.04}$
$B(M1; 1_3^+ \rightarrow 2_2^+)$	–	–

$2_2^+$  state has more than twice the strength of the corresponding transition in  $^{96}\text{Mo}$ . The MS excitations in  $^{96}\text{Mo}$  are weaker with greater fragmentation than those in  $^{94}\text{Mo}$ . Also evident is the  $\frac{B(M1; 1^+ \rightarrow 0_g^+)}{B(M1; 1^+ \rightarrow 2_2^+)}$  ratio, which increases from 38% in  $^{94}\text{Mo}$  to 81% in  $^{96}\text{Mo}$ . As we get further from single-particle-like nuclei, the MS excitations apparently become less well defined.

The  $B(M1)$  values have been compared with those obtained from photon scattering experiments in Ref. [25]; this comparison is shown in Table IV. In all cases of the  $1^+$  levels identified in the photon scattering work, we were able to find  $M1$  decays to levels other than the ground state. Thus the total  $B(M1)$  values for decays from these levels are larger than the values given in Ref. [25].

We, however, do not agree with the assignment in Ref. [25] of the  $1_3^+$  state at 3425 keV as a MS state. Even though the state does decay with a large  $B(M1)$  to the ground state, it lacks the signature of a U(5) or O(6) MS decay of a large  $B(M1)$  to the  $2_2^+$  level. This level does not decay to this or any other two-phonon state and, therefore, is not included in the assignment of  $1_{\text{ms}}^+$  excitations.

IBM-2 calculations were performed for  $^{96}\text{Mo}$  using a  $^{88}\text{Sn}$  core, with  $N_\pi = 2$  proton bosons and  $N_\nu = 2$  neutron bosons. Results for the U(5) and O(6) limits [40] were calculated using  $e_\pi = 8 e \text{ fm}^2$ ,  $e_\nu = 0$ ,  $g_\pi = 1$ , and  $g_\nu = 0$  and are displayed in Table V. These large values for the boson effective charges are in agreement with Ref. [6]. Calculations might indicate that this nucleus behaves better in the U(5) vibrational limit at low excitation energies ( $2_{\text{ms}}^+$ ) whereas the O(6) triaxial limit is more suitable at higher excitation energies ( $1_{\text{ms}}^+$ ).

TABLE V. Comparison of experimental data with IBM-2 calculations for U(5) and O(6) configurations. All  $B(M1)$  values are given in  $\mu_N^2$  and  $B(E2)$  values are in W.u., where 1 W.u. =  $26.11 e^2 \text{ fm}^4$  for the  $^{96}\text{Mo}$  nucleus. For the  $B(M1)$  experimental values, both the  $1^+$  levels at 2794 and 3300 keV contribute to the mixed-symmetry state and, therefore, were both included.

Observable	U(5)	O(6)	Expt.
$B(M1; 2_{\text{ms}}^+ \rightarrow 2_1^+)$	0.36	0.48	0.17(2)
$B(E2; 2_{\text{ms}}^+ \rightarrow 0_g^+)$	0	30	$0.08_{-0.01}^{+0.02}$
$B(M1; 1_{\text{ms}}^+ \rightarrow 0_g^+)$	0	0.19	$0.16_{-0.02}^{+0.03}$
$B(M1; 1_{\text{ms}}^+ \rightarrow 2_2^+)$	0.56	0.57	$0.18_{-0.03}^{+0.04}$

Smirnova *et al.* examined the  $M1$  transitions from  $^{94}\text{Mo}$  in both the  $U(5)$  and  $O(6)$  limits in the IBM-2 model [41]. They concluded that  $^{94}\text{Mo}$  is transitional between these limits but closer to the  $O(6)$  symmetry. Therefore,  $^{96}\text{Mo}$  may be even nearer to this limit with even weaker  $M1$  strength and a low-lying second  $0^+$  state.

## VII. CONCLUSION

Both one-phonon and two-phonon mixed-symmetry excitations are found in  $^{96}\text{Mo}$ , but they are more fragmented and more difficult to identify than the corresponding well-characterized excitations in  $^{94}\text{Mo}$ . Indeed, without the systematics of excitations in  $^{92}\text{Zr}$ ,  $^{94}\text{Mo}$ , and  $^{96}\text{Ru}$  as guides, these states in  $^{96}\text{Mo}$  would have been difficult to identify.

The presence of strong  $M1$  transitions from the two-phonon  $1^+$  MS excitation to the ground state suggests quite clearly

that we are not dealing with  $U(5)$  symmetry in either  $^{94}\text{Mo}$  or the present nucleus,  $^{96}\text{Mo}$ . Such  $M1$  excitations are forbidden in that symmetry. Instead, an  $O(6)$  symmetry representation seems to be most realistic.

Although  $O(6)$  might well be the best description of symmetry at MS energies near 3 MeV, the presence of one- and two-phonon fully symmetric levels suggests that  $U(5)$  does hold at lower energies below 1.8 MeV excitation energy. Clearly, the identification of MS excitations together with symmetric excitations provides sensitive tests of nuclear structure.

## ACKNOWLEDGMENTS

We thank H. E. Baber for his help with accelerator maintenance and operation. We gratefully acknowledge discussions with N. Warr, P. E. Garrett, and N. Pietralla. This material is based upon work supported by the U.S. National Science Foundation under Grant No. PHY-0354656.

- 
- [1] P. H. Regan, A. D. Yamamoto, F. R. Xu, C. Y. Wu, A. O. Macchiavelli, D. Cline, J. F. Smith, S. J. Freeman, J. J. Valiente-Dobón, K. Andgren *et al.*, Phys. Rev. C **68**, 044313 (2003).
- [2] J. Skalski, S. Mizutori, and W. Nazarewicz, Nucl. Phys. **A617**, 282 (1997).
- [3] Evaluated Nuclear Structure Data File, National Nuclear Data Center, Brookhaven National Laboratory, Long Island, NY (2005).
- [4] N. Pietralla, C. Fransen, P. von Brentano, A. Dewald, A. Fitzler, C. Friessner, and J. Gableske, Phys. Rev. Lett. **84**, 3775 (2000).
- [5] C. Fransen, N. Pietralla, P. von Brentano, A. Dewald, J. Gableske, A. Gade, A. Lisetskiy, and V. Werner, Phys. Lett. **B508**, 219 (2001).
- [6] C. Fransen, N. Pietralla, Z. Ammar, D. Bandyopadhyay, N. Boukharouba, P. von Brentano, A. Dewald, J. Gableske, A. Gade, J. Jolie *et al.*, Phys. Rev. C **67**, 024307 (2003).
- [7] A. Arima, T. Otsuka, F. Iachello, and I. Talmi, Phys. Lett. **B66**, 205 (1977).
- [8] T. Otsuka, A. Arima, and F. Iachello, Nucl. Phys. **A309**, 1 (1978).
- [9] F. Iachello, Phys. Rev. Lett. **53**, 1427 (1984).
- [10] D. Bohle, A. Richter, W. Steffen, A. E. L. Dieperink, N. LoIudice, F. Palumbo, and O. Scholten, Phys. Lett. **B137**, 27 (1984).
- [11] A. Richter, Prog. Part. Nucl. Phys. **34**, 261 (1995).
- [12] U. Kneissl, H. H. Pitz, and A. Zilges, Prog. Part. Nucl. Phys. **37**, 349 (1996).
- [13] V. Werner, D. Belic, P. von Brentano, C. Fransen, A. Gade, H. von Garrel, J. Jolie, U. Kneissl, C. Kohstall, A. Linneman *et al.*, Phys. Lett. **B550**, 140 (2002).
- [14] N. Pietralla, C. J. Barton, III, R. Krucken, C. W. Beausang, M. A. Caprio, R. F. Casten, J. R. Cooper, A. A. Hecht, H. Newman, J. R. Novak, and N. V. Zamfir, Phys. Rev. C **64**, 031301(R) (2001).
- [15] H. Klein, A. F. Lisetskiy, N. Pietralla, C. Fransen, A. Gade, and P. von Brentano, Phys. Rev. C **65**, 044315 (2002).
- [16] J. N. Orce, J. D. Holt, A. Linnemann, C. J. McKay, S. R. Leshner, C. Fransen, J. W. Holt, A. Kumar, N. Warr, V. Werner, J. Jolie, T. T. S. Kuo, M. T. McEllistrem, N. Pietralla, and S. W. Yates, Phys. Rev. Lett. **97**, 062504 (2006).
- [17] D. Heck, N. Ahmed, U. Fanger, W. Michaelis, H. Ottmar, and H. Schmidt, Nucl. Phys. **A159**, 49 (1970).
- [18] J. Barrette, M. Barrette, A. Boutard, R. Haroutunian, G. Lamoureux, G. Renaud, and S. Monaro, Nucl. Phys. **A172**, 41 (1971).
- [19] S. K. Basu and A. P. Patro, Nucl. Phys. **A171**, 231 (1971).
- [20] S. J. Burger and G. Heymann, Nucl. Phys. **A243**, 461 (1975).
- [21] E. Fretwurst, G. Lindström, K. F. von Reden, V. Riech, S. I. Vasiljev, P. P. Zarubin, O. M. Knyazkov, and I. N. Kuchkina, Nucl. Phys. **A468**, 247 (1987).
- [22] A. Moalem, M. A. Moinester, J. Alster, and Y. Dupont, Nucl. Phys. **A196**, 605 (1972).
- [23] A. B. Smith, P. Guenther, and J. Whalen, Nucl. Phys. **A244**, 213 (1975).
- [24] M. T. McEllistrem, J. D. Brandenberger, K. Sinram, G. P. Glasgow, and K. C. Chung, Phys. Rev. C **9**, 670 (1974).
- [25] C. Fransen, N. Pietralla, A. P. Tonchev, M. W. Ahmed, J. Chen, G. Feldman, U. Kneissl, J. Li, V. N. Litvinenko, B. Perdue *et al.*, Phys. Rev. C **70**, 044317 (2004).
- [26] P. E. Garrett, N. Warr, and S. W. Yates, J. Res. Natl. Inst. Stand. Technol. **105**, 141 (2000).
- [27] V. C. Rogers and E. Sheldon, Comput. Phys. Commun. **6**, 99 (1973).
- [28] P. E. Garrett, H. Lehmann, J. Jolie, C. A. McGrath, M. Yeh, W. Younes, and S. W. Yates, Phys. Rev. C **64**, 024316 (2001).
- [29] T. Belgya, G. Molnár, and S. W. Yates, Nucl. Phys. **A607**, 43 (1996).
- [30] K. B. Winterbon, Nucl. Phys. **A246**, 293 (1975).
- [31] A. I. Vdovion, Ch. Stoyanov, and W. Andrejtscheff, Nucl. Phys. **A440**, 437 (1985).
- [32] L. K. Peker, Nucl. Data Sheets **68**, 165 (1993).
- [33] H. W. Taylor, B. Singh, R. J. Cox, and A. H. Kukoc, Z. Phys. **239**, 42 (1970).
- [34] C. M. Lederer, J. M. Jaklevic, and J. M. Hollander, Nucl. Phys. **A169**, 449 (1971).
- [35] S. Monaro, J. Barrette, and A. Boutard, Can. J. Phys. **46**, 2375 (1968).

- [36] E. R. Flynn, F. Ajzenberg-Selove, R. E. Brown, J. A. Cizewski, and J. W. Sunier, *Phys. Rev. C* **24**, 2475 (1981).
- [37] V. Werner, Masters thesis, University of Cologne, 2000 (unpublished).
- [38] S. Antman, Y. Grunditz, A. Johansson, B. Nyman, H. Pettersson, and B. Svahn, *Z. Phys.* **233**, 275 (1970).
- [39] A. Bohr and B. R. Mottelson, *Nuclear Structure*, Vol. II (Benjamin, Elmsford, NY, 1975), p. 326.
- [40] P. van Isacker, K. Heyde, J. Jolie, and A. Sevrin, *Ann. Phys. (NY)* **171**, 253 (1986).
- [41] N. A. Smirnova, N. Pietralla, A. Leviatan, J. N. Ginocchio, and C. Fransen, *Phys. Rev. C* **65**, 024319 (2002).